HHS Public Access

Author manuscript

Nat Neurosci. Author manuscript; available in PMC 2015 August 01.

Published in final edited form as:

Nat Neurosci. 2015 February ; 18(2): 262–271. doi:10.1038/nn.3920.

Visual recognition memory, manifest as long-term habituation, requires synaptic plasticity in V1

Sam F. Cooke[1,2,3], **Robert W. Komorowski**[1,2,3], **Eitan S. Kaplan**[1,2,3], **Jeffrey P. Gavornik**[1,2,3,4], and **Mark F. Bear**[1,2,3]

[1]Howard Hughes Medical Institute

[2]Picower Institute for Learning and Memory

[3]Department of Brain and Cognitive Sciences, Massachusetts Institute of Technology, 77, Massachusetts Avenue, Cambridge, Massachusetts, US, 02139

[4]Department of Biology, Boston University, 24 Cummington Mall, Boston, MA, 02215, USA

Abstract

Familiarity with stimuli that bring neither reward nor punishment, manifested through behavioural habituation, enables organisms to detect novelty and devote cognition to important elements of the environment. Here we describe in mice a form of long-term behavioural habituation to visual grating stimuli that is selective for stimulus orientation. Orientation-selective habituation (OSH) can be observed both in exploratory behaviour in an open arena, and in a stereotyped motor response to visual stimuli in head-restrained mice. We show that the latter behavioural response, termed a vidget, requires V1. Parallel electrophysiological recordings in V1 reveal that plasticity, in the form of stimulus-selective response potentiation (SRP), occurs in layer 4 of V1 as OSH develops. Local manipulations of V1 that prevent and reverse electrophysiological modifications likewise prevent and reverse memory demonstrated behaviourally. These findings suggest that a form of long-term visual recognition memory is stored via synaptic plasticity in primary sensory cortex.

Introduction

The cerebral cortex stores memory[1], but precisely how and where specific types of information are retained in the neocortex remains poorly understood. The minimal criteria necessary to conclude that experience-dependent modification of a particular cortical area is an essential substrate of learning and memory would include evidence that: (1) cortical electrophysiological responses are persistently modified by experiences that are encoded as

Author contributions

S.F.C designed all experiments, conducted experiments described in figures 1–2, 4, 6–8 and all supplemental figures, analyzed all data shown in figures 1–2, 4 and 6–8 and all supplemental figures and wrote the manuscript. R.W.K designed and conducted, analyzed and described all experiments shown in figure 5, as well as participating in analysis for figure 3. E.S.K. conducted experiments described in figures 2 and 7. J.P.G designed and conducted experiments in figure 3 and developed the stimulus generation and recording system for acquisition of data and participated in data analysis. M.F.B designed experiments and wrote the manuscript.

memory, (2) such modifications coincide with changes in behaviour that depend upon this cortical area, and (3) local manipulations of cortex that prevent or reverse electrophysiological modifications likewise prevent or reverse memory demonstrated behaviourally.

Previous studies in our laboratory have documented a robust and long-lasting potentiation of electrophysiologial responses in the primary visual cortex (V1) following the controlled exposure of head-fixed awake mice to high contrast visual grating stimuli[2]. The underlying synaptic mechanism of this response modification has been localized to V1[3]. Because the effect is highly selective for the features of the experienced stimulus (*e.g.*, grating orientation), the phenomenon has been termed stimulus-selective response potentiation (SRP). The current study was designed to determine the behavioural significance of SRP in V1.

Here we show that V1 activity is required for the expression of a quantifiable behavioural response to novel visual stimuli. We find that behavioural responses to grating stimuli, in both head-fixed and freely behaving mice, habituate in a stimulus-selective manner as SRP develops across days in V1, and that local V1 manipulations which prevent and reverse SRP do the same to stimulus-selective behavioural habituation. Taken together, our results support the conclusion that experience-dependent plasticity in primary visual cortex is a substrate for visual recognition memory, manifest behaviourally as long-term habituation to familiar stimuli.

Results

The vidget: Visually-driven behaviour in head-fixed mice

We developed an assay of visual detection based on our observation that head-fixed mice spontaneously fidget in response to visual stimuli. We call this response, induced with full-field, phase-reversing (2 Hz) sinusoidal grating stimuli, a “vidget” (visually-induced fidget) and measure it via a piezo-electric sensor located beneath the forepaws of restrained mice (Figure 1a, Video1). These vidgets were quantified as the average stimulus-locked voltage signal, rectified and normalized to a pre-stimulus baseline as shown in Figure 1b. We found that vidget onset latency, determined by the first time-point greater than one standard deviation above the pre-stimulus baseline in 75 stimulus onsets from 15 mice, is ~150 milliseconds (Figure 1c). The response to individual stimuli was variable, with approximately 30 % of trials failing to induce movement (Figure S1). Nevertheless all 15 mice had quantifiable responses above baseline by averaging 5 onsets per animal (Figure 1d). Unless otherwise stated, all subsequent behavioural data is reported as per subject averages with complete distributions shown in supplementary figures.

We next determined if this behaviour can be used to assess visual contrast sensitivity and acuity by simultaneously recording vidgets and visually evoked potentials (VEPs) in binocular layer 4 of V1, a surrogate measure of visual detection[3,4]. We presented 100-second blocks of grating stimuli at various contrasts and spatial frequencies to 15 implanted mice. High contrast stimuli evoked significantly larger vidgets than low contrast stimuli (Figure 1e) and low spatial frequencies elicited larger vidgets than high (Figure 1f).

Simultaneously recorded VEPs had a similar contrast sensitivity (Figure 1g) and spatial acuity (Figure 1h). Thus, the vidget serves as a behavioural metric of visual detection aligned with V1 electrophysiology. In all subsequent experiments, we used 5 blocks of 100 % contrast, 0.05 cycles per degree, full field grating stimuli, separated by 30 seconds of grey, for each session because these stimulus parameters yield large and reliable vidgets and VEPs.

The vidget requires activity within V1

Many reflexive behavioural responses to visual stimuli occur without V1[5]. We therefore locally suppressed cortical activity by micro-infusing the $GABA_A$ receptor agonist muscimol (4 nmol in 1 μl over 10 minutes in each hemisphere, Figure S2a–c) to test if the vidget requires V1. To confirm inactivation we recorded VEPs in 8 mice before and 30 minutes after muscimol infusions. We then waited 2 days for a full recovery from muscimol before infusing vehicle and recording VEPs again. Muscimol significantly reduced VEP magnitude (28.18 ± 7.46 μV) compared to pre-infusion (78.58 ± 14.16 μV) or vehicle (74.13 ± 21.55 μV)(Figure S2d). Muscimol also significantly reduced vidget magnitude (1.82 ± 0.39 a.u.) compared to pre-infusion (4.79 ± 0.73 a.u.) or vehicle treatment (5.01 ± 0.91 a.u.) (Figure S2e–f). Onset-by-onset analysis also revealed significant impact of muscimol treatment over control conditions (Figure S2g).

Pharmacological blockade of activity using muscimol lasts for an extended period and may spread beyond V1. In order to overcome these potential issues we transiently inactivated V1 by expressing channelrhodopsin-2 (ChR2) in putative fast-spiking interneurons using local delivery of an AAV viral vector (AAV5-EF1α-DIO-hChR2(H134R)-eYFP) into V1 of mice expressing Cre-recombinase only in parvalbumin+ cells (B6;129P2-*Pvalb*$^{tm1(cre)Arbr}$/J) (Figures 2a–e, S3a–b). Ten PV-Cre mice and 8 wild-type littermate control mice were infected bilaterally within lateral (binocular) V1 (see Methods for histological confirmation). VEP electrodes and optical fibres were also implanted. One month later, mice were presented with a sinusoidal grating stimulus of a single orientation (10 s blocks of stimuli). Using a laser, we delivered blue light (473 nm) into both hemispheres throughout half of the stimulus presentations, commencing 0.5 seconds prior to visual stimulus onset and terminating 0.5 seconds after stimulus offset. VEP magnitude was significantly suppressed during laser stimulation in the PV-Cre mice (207.90 ± 27.76 μV) compared to when the laser was off (292.28 ± 36.89 μV). This suppression was not observed in the wild-type littermate mice (VEP with laser on: 303.19 ± 32.68 μV; laser off: 290.16 ± 33.49 μV) demonstrating that suppression was due to ChR2-mediated activation of PV+ inhibitory cells (Figure 2f). Reduction in V1 activity also significantly impacted the vidget. Laser stimulation suppressed the vidget in the PV-Cre mice (1.26 ± 0.24 a.u.) relative both to the absence of laser (2.89 ± 0.39 a.u) and the littermate controls during laser (2.90 ± 0.63 a.u.) (Figure 2g–i). The impact of laser in WT controls was not significant (2.26 ± 0.57 a.u.). Analysis conducted per behavioural onset appears in Figure S3c–d. Overall, these results demonstrate that the vidget is driven through activity in V1.

Stimulus-selective response potentiation (SRP)

We next wished to determine if the vidget is modified as SRP develops in V1. SRP is a long-lasting potentiation of VEPs as a consequence of brief daily exposure to oriented grating stimuli[2] and bears all the hallmarks of Hebbian synaptic plasticity[3] and visual perceptual learning[6]. Following SRP induction, VEPs evoked by familiar grating orientations are significantly larger than those evoked by novel orientations.

Previous recordings of SRP have been limited to VEPs in layer 4 of V1. In addition to determining the behavioural correlates of SRP, we wished to better understand the modification of translaminar patterns of V1 activity. We therefore implanted laminar probes (16 recording sites separated by 50 μm spanning the depth of V1 (Figure 3a). After recovery and acclimation to head-fixation, mice viewed a sinusoidal grating stimulus of fixed orientation (X°) repeatedly over 6 days. On day-7, we pseudo-randomly interleaved blocks of the familiar stimulus (X°) with a novel oriented stimulus (X + 90°) while acquiring VEPs. We then performed current source density (CSD) analysis to determine the laminar flow of current sinks and sources through V1[7]. In response to each stimulus phase reversal, current sinks appeared with progressively longer latencies at different cortical depths, reflecting the spread of synaptic activity across the canonical cortical circuit (activation of thalamo-recipient layers 4 and 6, followed by layers 2/3 and then layer 5)[8]. A comparison of current sinks in response to familiar (X°) and novel (X + 90°) stimuli revealed that the layer 4 sink was greater in magnitude for familiar than novel stimuli, while the deep layer 6 sink remained unchanged as a result of stimulus familiarity (Figure 3b). Thus, while SRP is distributed within the cortical circuit, it is not uniform throughout V1. We have therefore restricted our recordings to layer 4 for the remainder of this study, as this is a major site of SRP expression.

Although SRP has previously been reported as a synaptic phenomenon we wished to determine its impact on the firing of single units within layer 4 because changes in neural firing would be necessary to support changes in behaviour. To do this we implanted 10 mice with bundles of 8 recording electrodes targeting layer 4 of binocular V1. After recovery, mice were subjected to a similar protocol to that described above, viewing a designated oriented stimulus (X°) repeatedly over 6 days. On test day-7 mice were again presented with this familiar stimulus pseudo-randomly interleaved with a novel orientation (X + 90°) and unit activity recorded from each electrode was averaged together for each animal. We found that peak firing rate to the familiar stimulus (13.39 ± 2.51 Hz) was significantly elevated above the response to the novel stimulus (5.81 ± 1.61 Hz; Student-Newman-Keuls post-hoc test, $q_{(9)} = 5.51$, $p = 0.001$) or grey screen (1.20 ± 0.21 Hz; Student-Newman-Keuls post-hoc test, $q_{(9)} = 8.86$, $p < 0.001$) (Figure 3c–d). Thus, both short-latency synaptic and neuronal activity in thalamo-recpient layer 4 is potentiated by experience.

SRP is accompanied by orientation-selective behavioural habituation

To document behavioural modification during SRP we acquired VEPs and vidgets evoked by an oriented stimulus (X°) presented repeatedly over 8 days in 19 mice. On day-9, blocks of X° were interleaved with blocks of a novel stimulus (X + 90°) to test orientation selectivity (Figure 4a). SRP was evident by day-2 (183.58 ± 19.42 μV) relative to day-1

(125.38 ± 16.20 μV, Figure 4b), and testing on day-9 confirmed the orientation-selectivity: The novel orientation evoked significantly lower magnitude VEPs (166.86 ± 19.34 μV) than the familiar orientation (289.83 ± 24.53 μV, Figure 4c).

Vidgets diminished as VEPs potentiated, and this was already significant by day-2 (3.24 ± 0.51 a.u.) relative to day-1 (4.14 ± 0.55 a.u.). This suppression saturated by day-8 (1.51 ± 0.15 a.u., Figures 4d, S4a). Comparisons across individual onsets also reveal significant difference between day-1 and day-2 (Figure S4c). On day-9, a novel stimulus orientation (X + 90°) evoked vidgets of significantly greater magnitude (3.21 ± 0.43 a.u.) than the familiar stimulus orientation (1.61 ± 0.23 a.u., Figures 4e, S4b, video1). Comparisons across stimulus onsets confirm this effect (Figure S4d). Thus, orientation-selective habituation (OSH) of the vidget occurs in parallel with SRP.

OSH in the freely moving mouse

Animals preferentially explore novel objects[9] and thereby demonstrate memory of familiar objects. To examine the possibility that a similar preference can be observed for a novel orientation, we developed an assay to measure the emergence of OSH in freely moving mice (Figure 5a-b, Video2). Mice (n = 18) explored an open field arena with two video monitors positioned on opposite ends. The monitors showed uniform grey over ~30 minute habituation sessions on 2 days. Over the next 8 days, mice were presented with 5 blocks of oriented, phase reversing grating stimuli (X°) on each day on each monitor in a pseudo-random (counterbalanced) sequence. Exploration was quantified as time spent actively moving (velocity > 5 cm/s) within the zone next to the stimulus. Exploration on day-1 was significantly influenced by the visual stimulus and mice spent more time exploring proximal to stimulus presentation, whether on the left (59.5 ± 0.97 %) or right (64.1 ± 0.73 %)(Figure 5c). Exploration bias was measured using a preference index (see methods). We observed preference for the previously viewed stimulus decrease significantly over 8 days as familiarity developed (Figure 5d).

On day-9, blocks of novel X + 90° and familiar X° stimuli were shown on each monitor, to test if OSH had occurred. Mice exhibited preference for the novel orientation whether it was presented on the left (65.8 ± 0.69 %) or the right (59.4 ± 0.65 %) side of the arena. No significant preference was observed for the familiar stimulus on the left (50.9 ± 0.77 %) or the right (53.1 ± 0.60 %). Overall, there was greater preference for the novel (0.28 ± 0.09) than the familiar stimulus (0.03 ± 0.17, Figure 5e–f). Thus, OSH occurs in freely moving mice.

We next head-fixed mice (n = 18) that had undergone free exploration of stimuli to determine if SRP of the VEP and OSH of the vidget had been induced by experience in the arena. The animals were presented with interleaved blocks of X°, which had been viewed over the previous 9 days and X + 90°, which they had just viewed for the first time, but only in the arena. SRP was clearly induced in V1 by the experience in the open field arena (Figure 5g), as VEPs evoked by the familiar visual stimulus (169.2 ± 71.4 μV) were significantly greater in magnitude than those evoked by the novel (100.8 ± 53 μV). Behaviour was also recorded in a sub-set of these mice (n = 12) and vidgets evoked by the familiar stimulus (2.77 ± 0.46 a.u.) were significantly lower in magnitude than the novel

(4.79 ± 0.76 a.u.), revealing that OSH transfers from free exploration to head-fixation (Figure 5h, S5a–b). Induction of SRP and OSH in both restrained and freely behaving mice indicates that V1-dependent behavioural modifications occur as stimuli become familiar, regardless of context.

OSH is eye-specific

SRP is eye-specific, consistent with extensive evidence that it is induced by synaptic modifications within V1[2,3]. To test if OSH is also eye-specific, we restricted presentation of one stimulus (X°) to the left eye and another stimulus (X + 90°) to the right eye over 8 days in 14 mice. On day-9, we interleaved blocks of each of these stimuli, along with blocks of a third completely novel stimulus (X + 45°, "true novel") shown to each eye independently (Figure 6a–b). Vidgets driven by the familiar stimulus were significantly reduced in magnitude (1.54 ± 0.26 a.u.) compared with vidgets driven by the stimulus novel-to-eye (2.58 ± 0.36 a.u.) or true novel (3.10 ± 0.50 a.u.). Vidgets driven by the true novel stimulus and that novel to the eye were not significantly different in magnitude (Figures 6c–d). There was a similar pattern of selective suppression for the stimulus familiar to the eye when analysis was performed across all stimulus onsets (Figure S6). Overall, these results show that OSH is input-specific and involves modification of a circuit in which information from the two eyes can be segregated.

We also assessed SRP in these mice. As anticipated, VEPs evoked by the stimulus familiar to the eye evoked VEPs of significantly greater magnitude (124.21 ± 15.29 μV) than either true novel (70.70 ± 9.71 μV) or novel-to-eye (77.02 ± 10.89 μV)(Figure 6e). Importantly, there was also no significant difference between VEPs driven by novel-to-eye and true novel, suggesting no transfer of SRP across eyes.

OSH and SRP require NMDA receptors in V1

SRP induction requires activation of NMDA receptors (NMDARs)[2]. To test whether OSH shares this mechanism, we locally knocked down the mandatory GRIN1 subunit in 1-month old GRIN1$^{fl/fl}$ mice (B6.129S4-*Grin1*^{tm2Stl}/J)[10,11] by expressing Cre recombinase using an AAV8 viral vector (AAV8-hSyn-GFP-Cre) bilaterally in V1. Infected cells were labelled with GFP to track the spread of infection. Control animals were GRIN1$^{fl/fl}$ littermate mice that received local infection of just GFP under the same promoter and in the same serotype (AAV8-hSyn-GFP)(Figure 7a–b). Three weeks after infection, head-fixed mice were shown 5 blocks of 100 phase reversals of the grating stimulus per day over 6 consecutive days, while recording VEPs and vidgets. On day-7, the now familiar stimulus (X°) and a novel stimulus (X + 90°) were pseudo-randomly interleaved to test for expression of both SRP and OSH. In comparison to control littermate mice, potentiation of VEPs over days was significantly impaired as a result of GRIN1 deletion in V1 (Figure 7c). Additionally, expression of SRP on day-7 was selectively disrupted by loss of NMDARs in V1, as VEPs evoked by familiar (113.73 ± 14.57 % baseline) and novel stimuli (100.84 ± 12.95 % baseline) were of similar magnitude after local expression of Cre in GRIN1$^{fl/fl}$ mice. In littermate controls, by contrast, the familiar stimulus evoked VEPs (188.83 ± 19.40 % baseline) of significantly greater magnitude than the novel (115.01 ± 14.58 % baseline), demonstrating SRP (Figure 7d). OSH was also selectively disrupted only in GRIN1$^{fl/fl}$ mice

in which Cre had been expressed. Vidgets of similar magnitude were evoked by familiar (2.64 ± 0.48 a.u.) and novel stimuli (3.21 ± 0.61 a.u.) in these mice whereas, in their control littermates, the familiar stimulus evoked vidgets (2.03 ± 0.65 a.u.) of significantly lower magnitude than the novel (6.92 ± 1.15 a.u.), demonstrating OSH expression (Figure 7e–f). This same selective deficit in OSH in the Cre-expressing GRIN1$^{fl/fl}$ mice was observed when comparisons were made across all stimulus onsets (Figure S7a–b). These data support the conclusion that NMDAR within V1 are required for both SRP and OSH.

Acute blockade of NMDAR prevents acquisition of OSH

Our GRIN1 local knockdown strategy resulted in a chronic loss of NMDAR function in V1, which could potentially impair memory recall as well as learning. To address this concern we conducted an experiment in which we bilaterally infused the NMDAR antagonist AP5 (5 nmol in 1 μl, delivered over 10 min in each hemisphere) or vehicle into V1 of 18 mice prior to stimulus delivery. A crossover experimental design was employed in which mice were divided into 2 groups of 9. One group received infusions of vehicle and the other AP5 30 minutes before viewing an oriented stimulus (X°). After a day of rest to allow complete drug washout we tested whether OSH was present by showing interleaved blocks of X° and a novel stimulus (X + 90°). After a further day's rest, each group then received the opposite drug treatment before viewing another novel stimulus (X + 25°). On day-7, allowing another rest day for drug washout, we tested for OSH by presenting interleaved blocks of X + 25° and a final novel oriented stimulus (X + 115°, Figure 8a).

Vidgets to novel stimuli were significantly greater in magnitude (5.59 ± 0.56 a.u) than those to familiar stimuli following vehicle treatment (2.72 ± 0.43 a.u.) demonstrating OSH (Figure 8b). In contrast, the same mice did not discriminate the previously viewed stimulus (4.16 ± 0.68 a.u.), from novel (4.97 ± 0.52 a.u., Figure 8c) following AP5 treatment. Significant OSH was apparent in a comparison across stimulus onsets, although discrimination of familiar and novel stimuli was restricted to post-vehicle sessions (Figure S8c–d). Thus, blockade of NMDAR within V1 prevented OSH.

It is possible that NMDAR blockade impeded OSH by reducing activity in V1 and preventing information flow to the site of storage elsewhere. With this question in mind we compared the magnitude of VEPs evoked in the presence of AP5 (67.93 ± 10.81 μV) and vehicle (59.82 ± 7.06 μV) and found no difference between treatments (Figure S8a). We also confirmed that SRP did not occur under AP5. Within discrimination sessions after AP5, VEPs driven by the previously viewed stimulus (57.71 ± 8.53 μV) did not differ significantly from those evoked by novel (57.43 ± 7.31 μV). In contrast, familiar stimuli evoked VEPs of significantly greater magnitude (76.17 ± 10.02 μV) than novel (58.95 ± 7.61 μV) under vehicle treatment. Familiar stimuli experienced previously under vehicle also evoked VEPs of significantly greater magnitude than those experienced under AP5 (Figure S8b). Thus, blockade of NMDAR local to V1 prevents both SRP and OSH.

ZIP in V1 erases OSH

In order to test if OSH requires memory storage in V1 we applied ZIP (PKMzeta inhibitor peptide) after OSH had been saturated. This peptide has been shown to reverse LTP[12,13],

cortical memory[14] and SRP[3]. Mice (n = 36) underwent a typical OSH protocol over 8 days (Figure 8d). On day-9, blocks of the familiar X° stimulus and a novel X + 45° stimulus were interleaved. On day-10, half the mice (n = 18) were bilaterally infused with ZIP (10 nmol in 1 μl delivered over 10 min) while the other half (n = 18) received bilateral infusions of vehicle (1 μl delivered over 10 min). On day-11, blocks of the familiar X° stimulus and a second novel X + 90° stimulus were interleaved.

As previously reported[3], VEPs potentiated through induction of SRP returned to baseline levels after ZIP application in V1. VEPs driven by the familiar stimulus prior to ZIP application (145.00 ± 16.36 μV) dropped significantly in magnitude after ZIP application (97.53 ± 14.23 μV), and were no longer significantly different from those evoked by the novel stimulus (79.05 ± 8.23 μV, Figure S9a). Importantly, there was also a significant impact of ZIP on the expression of OSH. Prior to infusions, OSH was expressed (Figure 8e): the novel stimulus elicited vidgets of greater magnitude (4.47 ± 0.81 a.u.) than the familiar stimulus (2.32 ± 0.40 a.u.). On day-11, after infusions, a difference between the groups emerged. Significant discrimination of familiar (1.81 ± 0.18 a.u.) and novel stimuli (3.96 ± 0.50 a.u.) was maintained after vehicle (Figure 8f). However, after ZIP treatment mice failed to discriminate the novel (3.01 ± 0.53 a.u.) from the familiar stimulus (3.17 ± 0.76 a.u., Figure 8g, S9b–c). Thus, local infusion of ZIP into V1 disrupts established OSH, demonstrating that information supporting OSH is stored in V1.

Discussion

We have characterized a spontaneous, V1-dependent behaviour in the head-fixed mouse, termed the vidget, which accurately reports an animal's detection of novel visual stimuli. Over the course of days, vidgets gradually diminish in response to presentation of the same visual stimulus. Comparing the vidget response to familiar and novel stimuli reveals OSH. The orientation- and eye-specificity of this behavioural report of stimulus familiarity suggest that the neural mechanisms reside within V1. Consistent with this proposal, electrophysiological responses in V1 are selectively modified as OSH develops in head-fixed and freely moving mice. OSH is prevented by local V1 genetic ablation or temporary pharmacological blockade of NMDA receptors during visual experience. OSH is also reversed by local V1 delivery of the ZIP peptide. Taken together, our findings indicate that plasticity within V1 is required for both learning and long-term storage of visual recognition memory.

Measuring V1-dependent mouse vision with the vidget

The mouse has gained popularity as a species to study the neurobiology of vision and visual cortical plasticity, but it has been challenging to assay V1-dependent vision with behaviour. Previous attempts have involved operant conditioning or optokinetic reflexes[5,15,16]. However, operant conditioning is necessarily limited to specific stimulus sets and requires extensive training[17]; and optokinetic reflexes do not require participation of V1[18]. The properties of the vidget therefore offer some advantages as a simple assay of mouse vision. The vidget is elicited by presentation of visual grating stimuli without pre-training, and is abolished by inactivation of V1 with a number of methods. Vidgets are easily quantified and

reliably elicited using only a few blocks of stimuli (≤ 5). Vidgets and V1 VEPs show parallel decrements as stimulus contrast is decreased and spatial frequency is increased, and visual detection thresholds estimated by both methods are comparable. Furthermore, the fact that the vidget is measured in head fixed mice enables precise control of stimulus attributes, and also makes it compatible with simultaneous recordings of V1 activity.

We initially were concerned that the vidget might be a response to stimuli the mice find aversive, raising the possibility that mice actually detect low contrast stimuli but fail to respond because they find them less aversive than high contrast stimuli. Arguing against this interpretation are the simultaneous recordings of V1 VEPs, which disappear into the noise at the same contrasts as the vidgets. Furthermore, the reactions of the mice in the open field to presentation of the same high-contrast full-field stimuli are more compatible with the view that the vidget reflects an orienting response to novel stimuli the animals find interesting and worthy of exploration.

Because the vidget is a response to novel stimuli that does not require pre-training, it has the potential to be used in longitudinal studies of mouse vision, for example, after periods of monocular deprivation. The obvious complication is OSH. However, like VEPs, vidgets of comparable magnitude can be elicited in naïve mice with many different grating orientations. Thus, repeated measures of visual function should be possible without the complication of habituation as long as different stimuli are used.

Long-term behavioural habituation occurs via synaptic plasticity in V1

Familiarity with stimuli that bring neither reward nor punishment, manifested through behavioural habituation, enables organisms to devote cognition to important elements of the environment. Here we describe a form of long-term habituation in the mouse that enables detection of novel visual stimuli. We find that freely behaving mice actively explore novel visual gratings, and that behavioural habituation occurs as these stimuli become familiar. The orientation-selective behavioural habituation in the open field transfers to the vidget responses in the head-fixed mouse. Using the head-fixed mouse preparation, we have been able to identify the locus and some mechanistic requirements of OSH.

Behavioural expression of the vidget requires V1, and several converging lines of evidence suggest that a mechanism contributing to OSH also resides within V1. First, vidget habituation is eye-specific as well as orientation selective. Although these properties do not rule out other cortical areas[19], they are consistent with a V1 locus[20,21]. Second, local genetic knockdown of NMDA receptors in V1 or AP5 microinfusion prevents induction of OSH. These results show that activation of V1 neurons is required for OSH, and suggest a critical involvement of NMDA receptors in the synaptic mechanism. We cannot exclude the possibility that AP5 infusion during learning interrupts the flow of information to other cortical areas where the information is stored, but we note that this treatment did not suppress the V1 VEP. Third, expression of OSH is disrupted by local V1 infusion of ZIP. Although the data do not allow us to conclude that treated mice respond to familiar stimuli as if they were novel, the results clearly indicate that vidget responses fail to discriminate familiar and novel stimuli after ZIP infusion confined to V1.

ZIP was developed to selectively inhibit protein kinase M zeta (PKMζ), which has been implicated in the mechanism for stable expression of long-term synaptic potentiation (LTP) at many synapses[22]. Although it has been questioned whether PKMζ is the relevant target of ZIP[13,23], there is broad consensus that this peptide can reverse established LTP[13] and memory in a variety of neural systems[12,23,24], including the neocortex[14]. In mouse V1, previous work from our laboratory has shown that ZIP reverses SRP[3]. SRP is also prevented by local microinfusion of AP5 into V1, and is expressed by mechanisms shared with LTP. Findings that vidget habituation and SRP (1) are both induced by the same stimuli over the same time course, (2) have similar properties of orientation- and eye-specificity, and (3) are similarly sensitive to local V1 infusions of ZIP and AP5, together, strongly suggest these phenomena are closely related. We hypothesize that SRP is an electrophysiological consequence of synaptic modifications that contribute to OSH. The finding that selective visual experience that produces OSH in the open field also induces VEP potentiation supports this hypothesis.

Given that habituation features a decrement in behavioural response, it is intuitive to imagine synaptic depression as an underlying mechanism. Indeed, there is evidence for synaptic depression in some neural pathways displaying habituation[25–27]. However, a viable alternative is that the synaptic potentiation observed in SRP enforces a selective suppression of a separate response pathway. Given that inactivation of V1 prevents performance of the vidget, a logical extension of this hypothesis is that parallel pathways pass through V1: (1) a ‘response’ pathway that directly mediates the vidget and which does not undergo long-term modification and (2) a ‘learning’ pathway that is selectively strengthened through Hebbian plasticity and subsequently suppresses the output of the ‘response’ pathway. Although speculative, this proposal is anatomically plausible[8] and shares common features with influential theories of habituation[28–30].

We note that deficits in habituation are well documented in schizophrenia. These may contribute to the disrupted attention that characterizes the cognitive symptoms of the disorder[31]. Deficits in a physiological phenomenon similar to SRP have also been observed in individuals with schizophrenia[32]. Assays of SRP and OSH in mutant mice engineered to carry genetic disruptions linked to schizophrenia therefore have the potential to uncover aspects of cortical pathophysiology that could suggest new treatment strategies[33].

V1 as a cortical substrate for visual recognition memory

Although much experimental work has now revealed that primary sensory cortices retain the capacity for change in response to injury[34] or sensory deprivation[35,36], it has previously been unclear to what degree they encode memory resulting from everyday experience. We have shown here that plasticity in V1 contributes to memory. The observation that OSH transfers from free exploration of an arena to an apparatus in which the animal is restrained suggests that this plasticity supports context-independent recognition based on familiarity[37]. The perirhinal cortex, a higher-order visual region, is a major focus of work on familiarity[38] because this region is necessary for preferential exploration of novel objects[39]. Interestingly, novel object exploration requires mechanisms of synaptic long-term depression (LTD) in perirhinal cortex[40,41] and neuronal response to familiar objects is reduced in this region [42],

contrasting with SRP[2,3]. It will be interesting to determine in future studies how these representations of familiarity are related and whether V1 plasticity contributes to recognition of complex objects. Even in rodents, object recognition can be accomplished regardless of the viewpoint from which the object is observed[43], a property called invariance. OSH is not invariant because very simple stimuli are discriminated based simply on shifted orientation. Our findings suggest the possibility that low-level plasticity in V1 may serve as a building block for more complex representations contributing to invariant visual recognition memory.

On-line methods

Animals

All procedures were approved by the Committee on Animal Care at MIT, Cambridge, MA, USA and accorded with the guidelines of the National Institutes of Health. Mice were male C57BL/6 mice (Charles River laboratory international, Wilmington, MA) aged from P30–45. For optogenetic experiments mice expressing Cre recombinase directed by the parvalbumin promoter were used (B6;129P2-*Pvalb*$^{tm1(cre)Arbr}$/J – Jackson laboratory, ME, US. For local NMDAR knockdown experiments GRIN$^{fl/fl}$ mutant mice were used (B6.129S4-*Grin1*^{tm2Stl}/J – Jackson laboratory). In all cases mice were housed in groups of 2–5 with food and water available *ad libitum* and maintained on a 12 hour light-dark cycle. All mice participated only in the individual experiment described and did not undergo any prior or future experimental treatment or procedure.

Electrode/cannula implantation

Mice were anaesthetized with an intraperitoneal (i.p.) injection of 50 mg/kg ketamine and 10 mg/kg xylazine for surgery. 1 % lidocaine hydrochloride anesthetic was injected under the scalp of the mouse prior to incision. 0.1 mg/kg Buprenex was delivered sub-cutaneously for analgesia. The skull was cleaned with iodine and 70 % ethanol. A steel headpost was affixed to the skull anterior to bregma using cyanoacrylate glue. Burr holes (< 0.5 mm) were then drilled in the skull over binocular V1 (3.2 mm lateral of lambda). Tungsten electrodes (FHC, Bowdoinham, ME, US), 75 μm in diameter at their widest point, were implanted in each hemisphere, 450 μm below cortical surface. Silver wire (A-M systems, Sequim, WA, US) reference electrodes were placed over prefrontal cortex. For layer-specific analysis, linear silicon probes (16 recording sites, 50 μm spacing, NeuroNexus, Ann Arbor, MI, US) were implanted with the most superficial recording site just below the cortical surface. For unit recordings, custom-made bundles (tungsten H-Formvar wire, 20 μm outer diameter, California Fine Wire Company, Grover Beach, CA, US) were implanted 450 μm below the cortical surface. For local drug infusions, mice were also implanted bilaterally with 26 GA guide cannulae (Plastics One, Roanoke, VA, US), positioned lateral (3.5 mm lateral to lambda) to the recording site at a 45° angle to the recording electrode, 0.1 mm below surface. All implants were secured in place using cyanoacrylate glue. Finally, dental cement was applied to form a stable, protective head-cap. Dummy cannulae were inserted into guides. Mice were monitored postoperatively for signs of discomfort and allowed 24 hr for recovery.

Stimulus presentation

Visual stimuli were generated using custom software written in Matlab (MathWorks) using the PsychToolbox extension (http://psychtoolbox.org) to control stimulus drawing and timing. The display was positioned 20cm in front of the mouse and centred, thereby occupying 92° × 66° of the visual field. Mean luminance was 27cd/m^2. Visual stimuli consisted of full-field sinusoidal grating stimuli phase reversing at a frequency of 2Hz. Grating stimuli spanned the full range of monitor display values between black and white, with gamma-correction to ensure constant total luminance in both grey-screen and patterned stimulus conditions. For most experiments described, each stimulus block consisted of 200 phase reversals with 30-second intervals between each stimulus presentation, during which the screen was grey but of equivalent luminance. The one exception to this paradigm was the opto-genetic experiment (Figure 2), in which stimulus blocks were just 20 phase reversals long in order to minimize the required time for each laser pulse delivery. Stimulus orientation varied such that a novel orientation was always a minimum of 25° different from any experienced previously by the individual subject[3] and was never within 20° of horizontal because these orientations are known to elicit VEPs of greater magnitude than vertical or oblique stimuli. If more than 1 orientation was shown within a session, stimuli were pseudo-randomly interleaved such that 3 consecutive presentations of the same stimulus never occurred. For acuity experiments stimuli ranged across 0.05, 0.15, 0.3, 0.45, 0.6 and 1cycle/°. In these experiments stimulus contrast was fixed at 100 %. For contrast sensitivity experiments stimuli ranged across 1.5, 3.125, 6.25, 12.5, 25, 50 and 100 % contrast. In these experiments spatial frequency was fixed at 0.05cycle/°. Again, these stimuli were pseudo-randomized. Because of the large number of stimuli within these acuity and contrast sensitivity experiments, 2 separate sessions were used, each containing 5 blocks of each frequency or contrasts. Novel orientations were used for each acuity and contrast sensitivity session.

Head-fixed behaviour

All behavioural experiments were performed during the mouse subject's light cycle. A piezoelectrical recording device (C.B. Gitty, Barrington, NH, USA) was placed under the forepaws of head-restrained mice during all sessions. Mice became accustomed to the apparatus by sitting *in situ* in front of a grey screen for a 30-minute session on each of 2 days. Before stimulus presentation mice also underwent 5 min of grey screen presentation. A continuous voltage signal was recorded from the piezo for the entire session. Movements were detected as a shift in the voltage signal. The recording system was automated so that no one was ever present in the closed room for any of the recording period and white noise was played at 67 dB in order to mask outside noise.

For vidget scoring, the continuous voltage signal was down-sampled to 100 Hz. The period of interest in the experiments described here lasted from 2 seconds prior to stimulus onset until 5 seconds after stimulus onset (which was the first 10 phase reversals in a block). For the eye-specific experiments the measurement was limited to 2 seconds after stimulus onset as vidgets were of lower magnitude. Quantification of movement driven by the onset of the stimulus (the vidget) was calculated by taking the Root Mean Square (SQRT (X^2)) of the voltage signal. Post-stimulus signal was then normalized to the average magnitude during

the 2-second period prior to stimulus onset. The average normalized magnitude across the 5-second period subsequent to stimulus presentation was then used to quantify the degree of stimulus-driven movement and this is described throughout in arbitrary units (a.u.).

Freely-moving behaviour

The freely moving assay was conducted within a 40 x 40 x 30 cm square arena. 2 opposing walls were clear, allowing the mouse to view the stimulus monitors, whereas the other 2 walls and floor were occluded to minimize reflections and external visual cues. A black curtain surrounded the arena. Cineplex software (Plexon inc.) was used to acquire video of the mice at a rate of 30 frames/second and to automatically track the mouse's location.

After mice recovered from electrode implantation they were permitted to freely explore the testing area for 2 days over ~30 min per session while both monitors presented full-fields of grey. Phase-reversing stimulus presentation began the next day. Each day consisted of 2 free-exploration sessions separated by ~1 hour, in which the mouse was returned to its home cage. Each session began with 5 min of full-field grey on both monitors, followed by presentation of the visual stimulus on 1 side of the arena (actual location of the visual stimulus was counterbalanced from day to day). The stimulus consisted of a 100 % contrast, sinusoidal grating that phase-reversed at a frequency of 2 Hz. The stimulus had a spatial frequency of 0.05 cycles/°, as calibrated from the centre of the testing arena. Visual stimuli were presented as 5 blocks of 100 phase-reversals per block with 30 seconds of grey screen during the inter-block-interval. For the second training session, the stimulus was presented on the opposite side of the arena, following the same protocol. This training paradigm was implemented for 8 days with a single oriented stimulus. Day-9 consisted of 4 training sessions, 2 using the now familiar orientation and 2 using an orthogonal novel orientation. Once again, the order of stimulus presentation was counterbalanced from mouse to mouse. Subsequently, the mouse was head-fixed for VEP/vidget recordings.

To measure each mouse's preference for the visual stimulus we split the testing arena into halves (zones) and quantified the amount of time the mouse spent within the zone near the visual stimulus versus the side near the grey screen. To limit our analyses only to periods of active exploration we quantified the mouse's location for periods where running velocity exceeded 5 cm/s. Side preferences were then quantified as the percentage of total exploration time spent within each zone. Preference for the stimulus zone was expressed as the ratio of time spent exploring within the zone closest to the stimulus minus the time spent within the opposite zone over total exploration time ((stimulus zone-opposite zone)/overall exploration).

Electrophysiological Data Acquisition and analysis

All data was amplified and digitized using the Recorder-64 system (Plexon Inc., Dallas, TX, US). Two recording channels were dedicated to recording EEG/VEPs from V1 in each implanted hemisphere and a third recording channel was reserved for the Piezo-electrical input carrying the behavioural information for the majority of experiments. Fields were recorded with 1 kHz sampling and a 500 Hz low-pass filter. All data was extracted from the binary storage files and analyzed using custom software written in C++ and Matlab. VEPs

were averaged across all phase reversals within a block and trough-peak difference measured during a 200-millisecond period from phase reversal. For experiments described in Figure 3, 16 separate channels were used for laminar probe LFP/VEP recordings, each dedicated to an individual recording site. Current source density (CSD) analysis measured sink and source magnitudes across all cortical layers by calculating the second spatial derivative of the averaged VEP responses to familiar and novel stimuli. For spike recordings, 8 separate channels were used, each dedicated to a single wire within the electrode bundle. Spiking activity was digitized with 25 kHz sampling and multi-unit spikes were isolated using Offline Sorter (Plexon Inc.).

Viral infections

All viruses used to locally infect V1 were adeno-associated viruses (AAV). For optogenetic experiments we infected V1 of ~1 month old mice expressing Cre recombinase directed by the parvalbumin promoter (B6;129P2-*Pvalb*$^{tm1(cre)Arbr}$/J – Jackson laboratory, ME, US) or wild-type littermates with AAV5-EF1α-DIO-hChR2(H134R)-eYFP (UNC viral core – generated by Dr. Karl Deisseroth's laboratory). Using a glass pipette and nanoject system (Drummond scientific, Broomall, PA, US) we delivered 81 nl of virus at each of 3 cortical depths: 600 μm, 450 μm and 300 μm below surface. At each depth 6 injections of 13.5 nl were delivered, each separated by 15 secs, and 5 mins was allowed between re-positioning for depth. For local GRIN1 knockdown, ~1 month old mice GRIN$^{fl/fl}$ mutant mice (B6.129S4-*Grin1*^{tm2Stl}/J – Jackson laboratory) were infected locally in V1 with either AAV8-hSyn-GFP-Cre (knockdown, UNC viral core) or AAV8-hSyn-GFP (control, UNC viral core – generated by Dr Bryan Roth's laboratory). Again, injections were made at multiple depths. In this case 10 injections of 13.5 nl were made for a total of 135 nl at 4 cortical depths: 600 μm, 450 μm, 300 μm and 150 μm below surface. As before, each injection was separated by 15 secs, and 5 mins was allowed between re-positioning for depth. Mice were allowed 4 weeks recovery for virus expression to peak before experiments were initiated.

Optogenetics

After viral infection mice were also bilaterally implanted with VEP recording electrodes positioned in layer 4. Ready-made optic fibres (200 μm girth) mounted in stainless steel ferrules (1.25 mm diameter, 2 mm fibre projection, Thor labs, Newton, NJ, US) were then implanted positioned lateral (3.5 mm lateral to lambda) to the recording site and at a 45° angle to the recording electrode, 0.1 mm below surface in each hemisphere. 1 month later, after peak of viral expression, mice were habituated to the head-fixation apparatus over 2 days before conducting optogenetic experiments. We delivered 11-second long continuous pulses of blue light (473 nm, 150 mW) into V1 using a laser (Optoengine LLC, Midvale, UT, US). These light pulses were delivered simultaneous to 50% of the 10-second long visual stimulus presentations, commencing 30 ms prior to visual stimulus onset and ending 30 ms after offset. Animals were sacrificed and perfused within a week after this experiment for histological analysis.

Drug infusions

Infusions of ZIP and AP5 were conducted blind to treatment. Prior to infusion experiments, during which mice became accustomed to the recording apparatus, dummy cannulae were removed and repositioned in order to prevent blockage. On the day of infusion, syringes and guide tubing, attached to 33 GA injection cannulae, were filled with distilled water, which was separated from the injected solution with an air bubble. Dummies were again removed and injection cannulae were inserted through guides and allowed to sit in place for 5 min before injection. If blockade prevented smooth infusion the animal was excluded from the study (10 animals were excluded for this reason prior to inclusion in any dataset). Using a KD scientific infusion pump, slight positive pressure was maintained on the syringe while inserting the injection cannulae in order to prevent blockage. The vehicle solution was aCSF (124 mM NaCl, 5 mM KCl, 1.25 mM Na_2PO_4, 26 mM $NaHCO_3$, 1 mM $MgCl_2$, 2 mM $CaCl_2$) stored and defrosted on the day of injection. Muscimol (4 mM, Sigma, St. Louis, MO), AP5 (5 mM, Tocris, Bristol, UK) and ZIP (myr-SIYRRGARRWRKL-OH, 10 mM, Sigma, St. Louis, MO) were infused at 6 μl/hour over 10 minutes to inject 1 μl. The resulting local quantities are described in the manuscript. Hemispheres were injected in sequence.

Histology

Mice were deeply anaesthetized with fatal plus (pentobarbital) and perfused with saline followed by 4 % paraformaldehyde in 0.1 M phosphate buffer. The brain was removed and post-fixed for 24h at room temperature. After fixation, the brain was sectioned into 60 μm coronal slices using a vibratome. For assessment of the spread of viral infusions we performed Hoechst and FluoroMyelin Red stains were performed. Slices were incubated with a permeabilization solution (0.2 % Triton X-100 in PBS) for 30 mins at room temperature and then with a staining solution (Hoechst 33342, Life Technologies, 1:10,000 and FluoroMyelin Red, Life Technologies, 1:100 in PBS) for 30 mins. Slices were washed three times with PBS and mounted. Fluorescence images were taken with a confocal fluorescence microscope (Olympus). The margins of V1 were determined using the established techniques of observing the pronounced increase in thickness of layer 4 [44–46] and of increased myelination demarcating primary sensory areas [47]. A description of this approach is described in Figure S10.

Immunohistochemistry

Mice were deeply anaesthetized with fatal plus (pentobarbital) and perfused with saline followed by 4 %paraformaldehyde in 0.1M phosphate buffer. The brain was removed and post-fixed for 24h at room temperature. After fixation, the brain was sectioned into 60 μm coronal slices using a vibratome. Slices were incubated with blocking solution (10 % fetal bovine serum in PBS with 0.2 % Triton X-100) for 1 hour at room temperature and then with anti-Parvalbumin mouse primary antibody (MAB1572, Millipore; 1:1,000) diluted in blocking solution overnight at 4 degrees Celsius. Slices were then washed three times with PBS and incubated with the secondary antibody for 1h at room temperature (Alexa594-conjugated anti-mouse IgG, Invitrogen, 1:500. Slices were washed three times with PBS and mounted with 49,6-diamidino-2 phenylindole (DAPI)-containing Vectashield (Vector

Laboratories). Fluorescence images were taken with a confocal fluorescence microscope (Olympus).

Statistical analyses

In the results section, all data is expressed as a mean ± standard error of the mean (S.E.M). Sigmaplot and SPSS were used for statistical analysis. For all experiments, normality of distribution and homogeneity of variation was tested. Parametric ANOVA (for multiple groups) or 2-tailed t-tests (for 2 groups) were performed when data passed these tests. Otherwise, non-parametric ANOVAs or t-tests on ranks were used. If ANOVAs yielded significance, Student-Newman-Keuls post-hoc tests with adjustment for multiple comparisons were applied for individual comparisons. Repeated measures ANOVAs or paired t-tests were applied for all within subject comparisons. For other comparisons unpaired ANOVAs or t-tests were used. Individual tests used are described in the results. $P < 0.05$ is used as a threshold for significance throughout but exact P values are given for all comparisons for which the P value is above 0.001, except for post-hoc tests conducted after non-parametric tests on ranks. No explicit statistical methods were used to predetermine sample sizes, but our sample sizes throughout are similar to or greater than those generally employed to assess mouse behaviour.

Supplementary Material

Refer to Web version on PubMed Central for supplementary material.

Acknowledgments

We thank Arnie Heynen, Alex Chubykin and Ben Auerbach for helpful scientific discussions. We also thank Erik Sklar and Emily Greene-Colozzi for technical assistance and Suzanne Meagher for invaluable administrative support.

Funding

This research was partly supported by the Howard Hughes Medical Institute, a grant from the National Eye Institute (RO1EY023037), and gifts from the Picower Institute Innovation Fund (PIIF) and the Picower Neurological Disorder Research Fund (PNDRF). We additionally acknowledge a JPB Foundation Fellowship to R.W.K., NIMH training grant 5T32MH074249 support of E.S.K, and NIMH grant K99MH099654 to J.P.G.

References

1. Lashley KS. Mass Action in Cerebral Function. Science. 1931; 73:245–254.10.1126/science.73.1888.245 [PubMed: 17755301]
2. Frenkel MY, et al. Instructive effect of visual experience in mouse visual cortex. Neuron. 2006; 51:339–349.10.1016/j.neuron.2006.06.026 [PubMed: 16880128]
3. Cooke SF, Bear MF. Visual experience induces long-term potentiation in the primary visual cortex. The Journal of neuroscience: the official journal of the Society for Neuroscience. 2010; 30:16304–16313.10.1523/JNEUROSCI.4333-10.2010 [PubMed: 21123576]
4. Porciatti V, Pizzorusso T, Maffei L. The visual physiology of the wild type mouse determined with pattern VEPs. Vision Res. 1999; 39:3071–3081. [PubMed: 10664805]
5. Douglas RM, et al. Independent visual threshold measurements in the two eyes of freely moving rats and mice using a virtual-reality optokinetic system. Vis Neurosci. 2005; 22:677–684.10.1017/S0952523805225166 [PubMed: 16332278]

6. Gilbert CD, Sigman M, Crist RE. The neural basis of perceptual learning. Neuron. 2001; 31:681–697. [PubMed: 11567610]
7. Mitzdorf U. Current source-density method and application in cat cerebral cortex: investigation of evoked potentials and EEG phenomena. Physiological reviews. 1985; 65:37–100. [PubMed: 3880898]
8. Constantinople CM, Bruno RM. Deep cortical layers are activated directly by thalamus. Science. 2013; 340:1591–1594.10.1126/science.1236425 [PubMed: 23812718]
9. Bevins RA, Besheer J. Object recognition in rats and mice: a one-trial non-matching-to-sample learning task to study 'recognition memory'. Nature protocols. 2006; 1:1306–1311.10.1038/nprot.2006.205 [PubMed: 17406415]
10. Carlen M, et al. A critical role for NMDA receptors in parvalbumin interneurons for gamma rhythm induction and behavior. Molecular psychiatry. 2012; 17:537–548.10.1038/mp.2011.31 [PubMed: 21468034]
11. Korotkova T, Fuchs EC, Ponomarenko A, von Engelhardt J, Monyer H. NMDA receptor ablation on parvalbumin-positive interneurons impairs hippocampal synchrony, spatial representations, and working memory. Neuron. 2010; 68:557–569.10.1016/j.neuron.2010.09.017 [PubMed: 21040854]
12. Pastalkova E, et al. Storage of spatial information by the maintenance mechanism of LTP. Science. 2006; 313:1141–1144.10.1126/science.1128657 [PubMed: 16931766]
13. Volk LJ, Bachman JL, Johnson R, Yu Y, Huganir RL. PKM-zeta is not required for hippocampal synaptic plasticity, learning and memory. Nature. 201310.1038/nature11802
14. Shema R, Sacktor TC, Dudai Y. Rapid erasure of long-term memory associations in the cortex by an inhibitor of PKM zeta. Science. 2007; 317:951–953.10.1126/science.1144334 [PubMed: 17702943]
15. Andermann ML, Kerlin AM, Reid RC. Chronic cellular imaging of mouse visual cortex during operant behavior and passive viewing. Front Cell Neurosci. 2010; 4:3.10.3389/fncel.2010.00003 [PubMed: 20407583]
16. Histed MH, Carvalho LA, Maunsell JH. Psychophysical measurement of contrast sensitivity in the behaving mouse. J Neurophysiol. 2012; 107:758–765.10.1152/jn.00609.2011 [PubMed: 22049334]
17. Shuler MG, Bear MF. Reward timing in the primary visual cortex. Science. 2006; 311:1606–1609.10.1126/science.1123513 [PubMed: 16543459]
18. Prusky GT, Silver BD, Tschetter WW, Alam NM, Douglas RM. Experience-dependent plasticity from eye opening enables lasting, visual cortex-dependent enhancement of motion vision. The Journal of neuroscience: the official journal of the Society for Neuroscience. 2008; 28:9817–9827.10.1523/JNEUROSCI.1940-08.2008 [PubMed: 18815266]
19. Marshel JH, Garrett ME, Nauhaus I, Callaway EM. Functional specialization of seven mouse visual cortical areas. Neuron. 2011; 72:1040–1054.10.1016/j.neuron.2011.12.004 [PubMed: 22196338]
20. Karni A, Sagi D. Where practice makes perfect in texture discrimination: evidence for primary visual cortex plasticity. Proceedings of the National Academy of Sciences of the United States of America. 1991; 88:4966–4970. [PubMed: 2052578]
21. Poggio T, Fahle M, Edelman S. Fast perceptual learning in visual hyperacuity. Science. 1992; 256:1018–1021. [PubMed: 1589770]
22. Sacktor TC. How does PKMzeta maintain long-term memory? Nat Rev Neurosci. 2011; 12:9–15.10.1038/nrn2949 [PubMed: 21119699]
23. Lee AM, et al. Prkcz null mice show normal learning and memory. Nature. 2013; 493:416–419.10.1038/nature11803 [PubMed: 23283171]
24. Serrano P, et al. PKMzeta maintains spatial, instrumental, and classically conditioned long-term memories. PLoS biology. 2008; 6:2698–2706.10.1371/journal.pbio.0060318 [PubMed: 19108606]
25. Groves PM, Thompson RF. Habituation: a dual-process theory. Psychol Rev. 1970; 77:419–450. [PubMed: 4319167]
26. Horn G. Neuronal mechanisms of habituation. Nature. 1967; 215:707–711. [PubMed: 6059539]
27. Glanzman DL, Thompson RF. Evidence against conduction failure as the mechanism underlying monosynaptic habituation in frog spinal cord. Brain Res. 1979; 174:329–332. [PubMed: 226221]

28. Sokolov EN. Higher nervous functions; the orienting reflex. Annu Rev Physiol. 1963; 25:545–580.10.1146/annurev.ph.25.030163.002553 [PubMed: 13977960]
29. Konorski, J. Integrative activity of the brain. University of Chicago Press; 1967.
30. Wagner, AR. Mechanisms of Learning and Motivation: A Memorial Volume for Jerry Konorski. Dickinson, A.; Boakes, RA., editors. Lawrence Earlbaum Associates; 1979. p. 53-82.
31. Braff DL, Swerdlow NR, Geyer MA. Gating and habituation deficits in the schizophrenia disorders. Clin Neurosci. 1995; 3:131–139. [PubMed: 7583619]
32. Cavus I, et al. Impaired visual cortical plasticity in schizophrenia. Biol Psychiatry. 2012; 71:512–520.10.1016/j.biopsych.2012.01.013 [PubMed: 22364738]
33. Cooke SF, Bear MF. Stimulus-selective response plasticity in the visual cortex: an assay for the assessment of pathophysiology and treatment of cognitive impairment associated with psychiatric disorders. Biol Psychiatry. 2012; 71:487–495.10.1016/j.biopsych.2011.09.006 [PubMed: 22019003]
34. Kaas JH, et al. Reorganization of retinotopic cortical maps in adult mammals after lesions of the retina. Science. 1990; 248:229–231. [PubMed: 2326637]
35. Sawtell NB, et al. NMDA receptor-dependent ocular dominance plasticity in adult visual cortex. Neuron. 2003; 38:977–985. [PubMed: 12818182]
36. Yoshida T, Ozawa K, Tanaka S. Sensitivity profile for orientation selectivity in the visual cortex of goggle-reared mice. PLoS One. 2012; 7:e40630.10.1371/journal.pone.0040630 [PubMed: 22792390]
37. Yonelinas AP. Components of episodic memory: the contribution of recollection and familiarity. Philosophical transactions of the Royal Society of London. Series B, Biological sciences. 2001; 356:1363–1374.10.1098/rstb.2001.0939 [PubMed: 11571028]
38. Murray EA, Bussey TJ. Perceptual-mnemonic functions of the perirhinal cortex. Trends Cogn Sci. 1999; 3:142–151. [PubMed: 10322468]
39. Albasser MM, et al. Separate but interacting recognition memory systems for different senses: the role of the rat perirhinal cortex. Learn Mem. 2011; 18:435–443.10.1101/lm.2132911 [PubMed: 21685150]
40. Griffiths S, et al. Expression of long-term depression underlies visual recognition memory. Neuron. 2008; 58:186–194.10.1016/j.neuron.2008.02.022 [PubMed: 18439404]
41. Barker GR, Bashir ZI, Brown MW, Warburton EC. A temporally distinct role for group I and group II metabotropic glutamate receptors in object recognition memory. Learn Mem. 2006; 13:178–186.10.1101/lm.77806 [PubMed: 16585793]
42. Xiang JZ, Brown MW. Differential neuronal encoding of novelty, familiarity and recency in regions of the anterior temporal lobe. Neuropharmacology. 1998; 37:657–676. [PubMed: 9705004]
43. Zoccolan D, Oertelt N, DiCarlo JJ, Cox DD. A rodent model for the study of invariant visual object recognition. Proceedings of the National Academy of Sciences of the United States of America. 2009; 106:8748–8753.10.1073/pnas.0811583106 [PubMed: 19429704]
44. Valverde F. Structural changes in the area striata of the mouse after enucleation. Experimental brain research. 1968; 5:274–292. [PubMed: 4889747]
45. Antonini A, Fagiolini M, Stryker MP. Anatomical correlates of functional plasticity in mouse visual cortex. The Journal of neuroscience: the official journal of the Society for Neuroscience. 1999; 19:4388–4406. [PubMed: 10341241]
46. van Brussel L, Gerits A, Arckens L. Identification and localization of functional subdivisions in the visual cortex of the adult mouse. The Journal of comparative neurology. 2009; 514:107–116.10.1002/cne.21994 [PubMed: 19260069]
47. Wang Q, Burkhalter A. Area map of mouse visual cortex. The Journal of comparative neurology. 2007; 502:339–357.10.1002/cne.21286 [PubMed: 17366604]

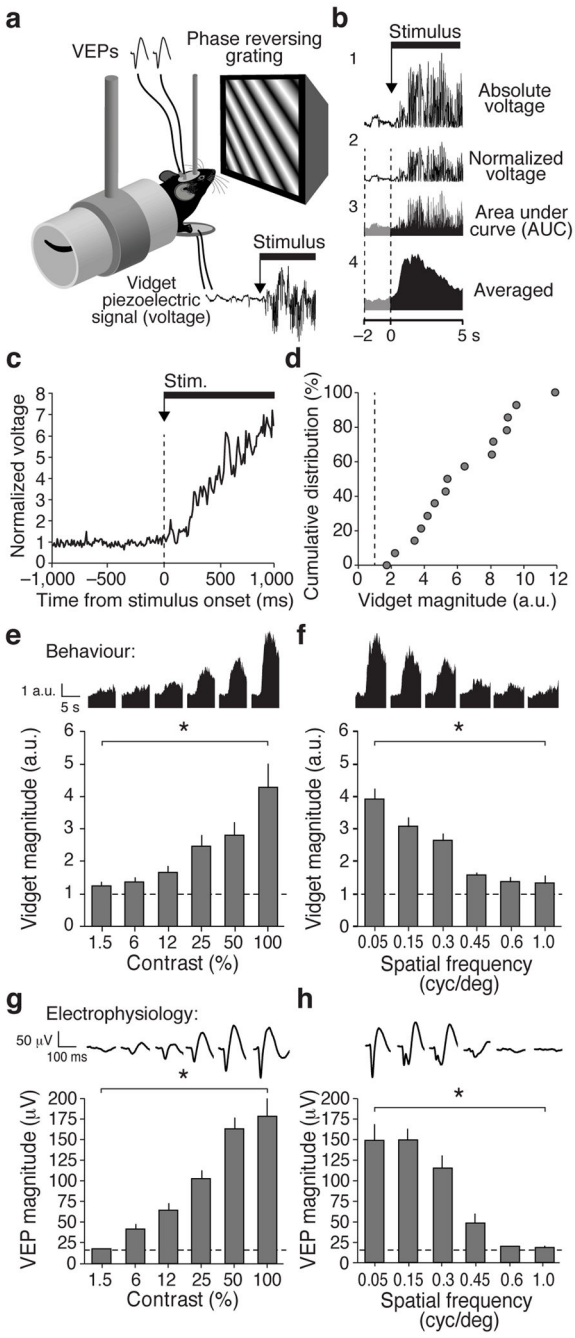

Figure 1. The Visually-induced fidget (vidget) reports visual detection

a) A piezoelectric disk was positioned under the forepaws of head-fixed, awake mice to record movements initiated by the onset of a full-field, phase-reversing, sinusoidal grating stimulus. In parallel, visual evoked potentials (VEPs) were recorded from the binocular zone of V1. **b**) Piezoelectric voltage signals were (1) rectified and (2) normalized to a 2-second pre-stimulus baseline period, indicated here by vertical dotted lines (see methods for details), and (3) quantified as the average magnitude over the first 5 seconds of stimulus presentation in arbitrary units (a.u.). The average vidget over multiple stimulus presentations

within a session provides an accurate measure of stimulus detection. **c**) The average vidget (15 mice, 75 stimulus presentations) shows a response latency of ~150 ms. **d**) Despite the variability across individual stimulus onsets, vidgets are observed in all mice. **e**) High contrast visual stimuli evoked greater magnitude vidgets than low contrast (n = 15 mice; Friedman 1-way repeated measures ANOVA on ranks, $X^2_{(5)} = 29.13$, $p < 0.001$). Averaged vidgets were taken from 10 stimulus blocks per contrast in each of 15 mice across a range of contrast values (spatial frequency was fixed at 0.05 cycles/° during varied contrast presentation). **f**) Sensitivity to varying spatial frequency was quantified in the same mice (contrast was fixed at 100 % during varied spatial frequency presentation). Low spatial frequency stimuli elicited greater magnitude vidgets than high spatial frequency (n = 15 mice; Friedman 1-way repeated measures ANOVA on ranks, $X^2_{(5)} = 44.91$, $p < 0.001$). Dashed line represents pre-stimulus baseline. Averaged vidgets including 2-second baselines are presented at the top of panels **e–f. g**) Averaged VEPs recorded in parallel reveal similar psychometric curve for contrast sensitivity to that observed with behaviour (n = 15; Friedman 1-way repeated measures ANOVA on ranks, $X^2_{(5)} = 68.83$, $p < 0.001$). **h**) VEP magnitude across a range of spatial frequencies also share a similar profile to the vidget (n = 15; Friedman 1-way repeated measures ANOVA on ranks, $X^2_{(5)} = 60.87$, $p < 0.001$). Dashed line represents noise levels. Averaged VEPs are displayed at top of panels **g–h**. Error bars represent S.E.Ms, asterisks denote significance of $p < 0.05$.

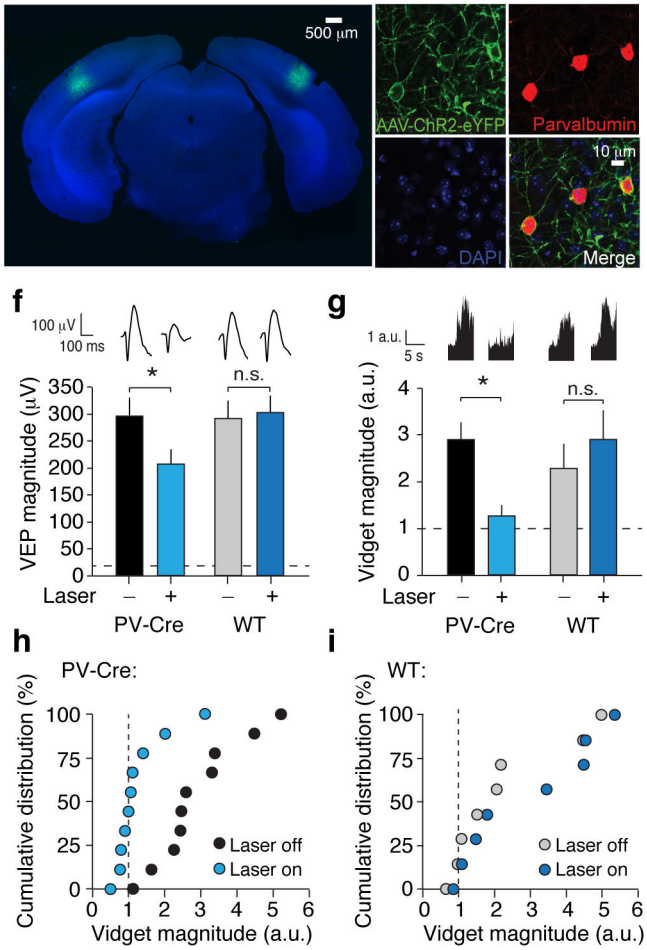

Figure 2. The vidget requires activity in V1

Optical fibres were implanted below the cortical surface targeting V1 and VEP electrodes positioned in layer 4. Light could then be delivered to the recording site *in vivo* while the animal views a visual stimulus and optogenetic strategies used to alter activity locally. By selectively expressing Channelrhodopsin2 (ChR2) in parvalbumin expressing (PV+) cells using Cre recombinase technology, blue light (473 nm) could be used to suppress activity in V1 through PV+ inhibition. **a**) An example coronal section through a mouse brain (DAPI stained) showing eYFP labelled cells (green) that express ChR2 bilaterally restricted to lateral (binocular) V1. **b**) Example histology showing eYFP label in select cortical cells expressing ChR2 (green). **c**) Immunoshistochemistry for parvalbumin reveals all those PV+ putative fast spiking interneurons (red) within the image in (**b**). **d**) DAPI label (blue) labels the nuclei of all cells in this region. **e**) eYFP+ cells are also PV+. Other DAPI+ cells (blue) are not co-labelled in green, demonstrating that they do not express ChR2. **f**) VEPs evoked by full-field sinusoidal grating stimuli were significantly suppressed in PV-Cre mice (n = 10) when blue light (473 nm) was applied using a laser (2-way repeated measures ANOVA: genotype x treatment interaction: $F_{(1,55)} = 13.395$; $p = 0.001$), measuring 207.90 ± 27.76 μV while the laser was on (light blue) and 292.28 ± 36.89 μV when it was off (black, n = 20 hemispheres; Student-Newman-Keuls post-hoc test, $q_{(19)} = 6.906$, $p < 0.001$). This

suppression was not observed in wild-type littermate mice (n = 8) infected with the same AAV5 virus, demonstrating that the laser had no impact without ChR2. In these animals VEPs measured 303.19 ± 32.68 μV when the laser was on (blue) and 290.16 ± 33.49 μV when it was off (grey, n = 16 hemispheres; Student-Newman-Keuls post-hoc test, $q_{(15)}$ = 0.866, p = 0.546). Averaged VEPs are presented at top of panel. Dashed line represents noise levels. **g**) Vidgets were significantly suppressed by blue light (473 nm) in the same PV-Cre mice (2-way repeated measures ANOVA: genotype x treatment interaction: $F_{(1,35)}$ = 6.639; p = 0.020). The vidget was suppressed in the PV-Cre mice (light blue, 1.26 ± 0.24 a.u.) relative both to the absence of laser (black, 2.89 ± 0.39 a.u.; n = 10 mice; Student-Newman-Keuls post-hoc test, $q_{(9)}$ = 3.919, p = 0.014) and littermate controls during laser (blue, 2.90 ± 0.63 a.u.; n = 8 mice; Student-Newman-Keuls post-hoc test, $q_{(16)}$ = 3.572, p = 0.017). Again, significant suppression of behaviour did not occur in WT mice relative to the absence of light application (grey, 2.26 ± 0.57 a.u.; n = 8 mice; Student-Newman-Keuls post-hoc test, $q_{(7)}$ = 1.384, p = 0.343). Averaged vidget responses are presented at top of panel. Dashed line represents pre-stimulus baseline. **h**) Cumulative distribution of averaged vidget per PV-Cre mouse pre-laser (black) and during laser (light blue). **i**) Cumulative distribution of averaged vidget per infected WT littermate mouse (n = 8) pre-laser (grey) and during laser (blue). Dashed line represents pre-stimulus baseline. Throughout figure error bars are S.E.Ms, asterisks denote significance of $p < 0.05$ and non-significant comparisons are denoted with n.s.

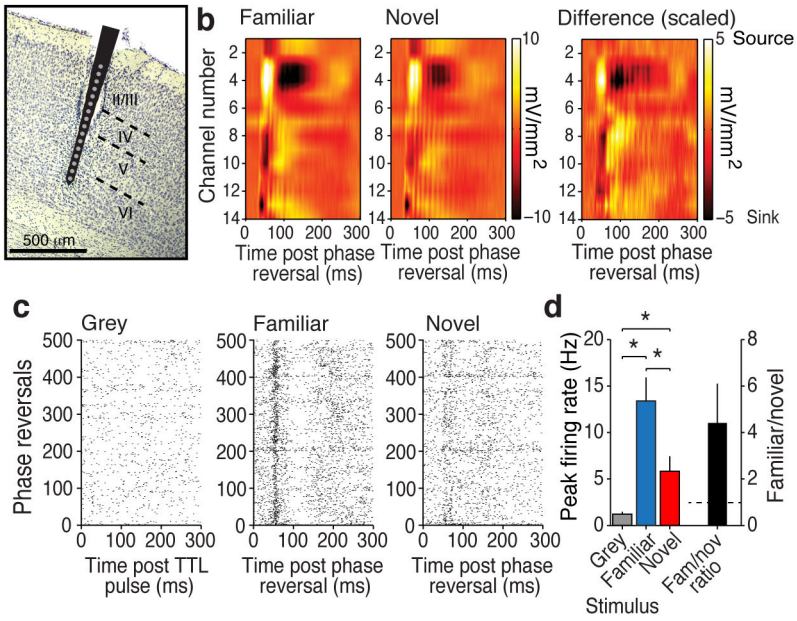

Figure 3. SRP is distributed but not uniform and impacts neural spiking

a) Example of a laminar probe implantation in mouse V1 with 16 recording sites separated by 50 μm increments. **b**) Current Source Densities (CSDs) were calculated from the local field potential (LFP) data and are presented for the familiar stimulus (left), the novel stimulus (middle) and a scaled subtraction of novel from familiar (right). Dark colours reflect current sinks and light colours current sources. **c**) Example raster plots showing multiunit firing from a single animal across the course of a familiarity test session in which familiar and novel oriented stimuli were pseudo-randomly interleaved and separated by viewing of a grey screen. In the left hand panel is the unit response to 30-second bouts of static grey stimuli interleaved between grating stimuli. This is presented arbitrarily time-locked for comparison with the phase reversing stimuli in the adjacent 2 panels. The middle panel shows the event-related response to each of 500 phase reversals across 5 blocks of a 2 Hz phase reversing familiar oriented stimulus. The right panel shows the event-related response to each of 500 phase reversals across 5 blocks of a 2 Hz phase reversing novel oriented stimulus. **d**) Summary plot of peak firing rate for multi-unit recordings across 10 mice. Peak firing after phase reversal is significantly elevated for the familiar stimulus (blue, 13.39 ± 2.51 Hz, n = 10; 1-way repeated measures ANOVA; $F_{(2,18)} = 20.01$, $p < 0.001$) relative to novel (red, 5.81 ± 1.61 Hz; Student-Newman-Keuls post-hoc test, $q_{(9)} = 5.51$, $p = 0.001$) and grey (grey, 1.20 ± 0.21 Hz; Student-Newman-Keuls post-hoc test, $q_{(9)} = 8.86$, $p < 0.001$). The ratio of peak firing rate to familiar/novel (black) is around 4.38 ± 1.71, indicating that, on average, the familiar stimulus evokes around 4 times greater peak firing rate than the novel. Error bars are SEMs. Asterisks denote significance of $p < 0.05$.

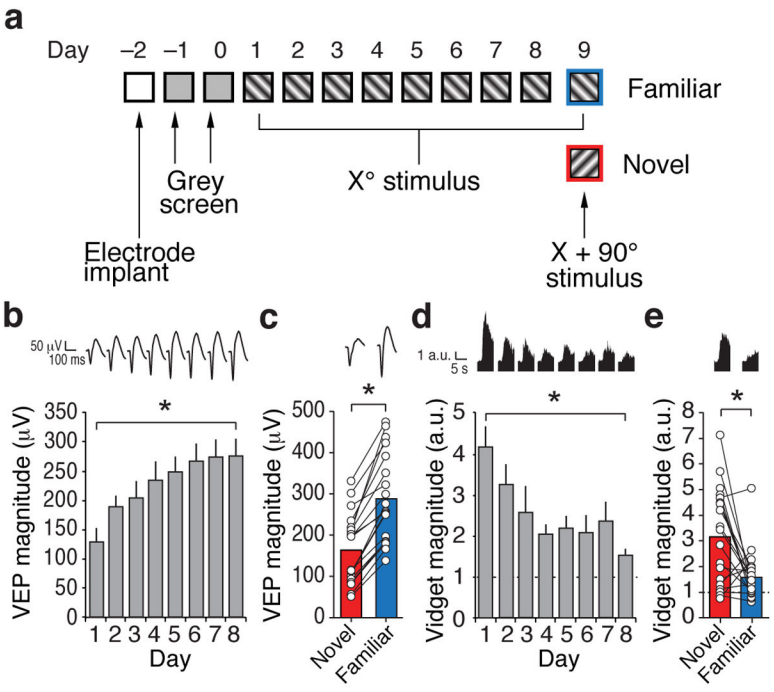

Figure 4. Orientation-selective habituation (OSH) occurs in parallel with stimulus-selective response potentiation (SRP)

a) Mice were implanted bilaterally in V1 with recording electrodes. Upon recovery they became accustomed to head-fixation for 2 days, viewing a grey screen. Over the next 8 days, mice were presented with 5 blocks of an X° oriented grating stimulus per day. On day-9, 5 blocks of the same stimulus were interleaved with 5 blocks of a novel orthogonal stimulus (X + 90°). **b**) VEPs underwent SRP (n = 19; Friedman 1-way repeated measures ANOVA on ranks, $X^2_{(7)} = 69.05$, $p < 0.001$), reaching significance by day-2 (183.58 ± 19.42 μV) relative to day-1 (125.38 ± 16.20 μV; Student-Newman-Keuls post-hoc test, $q_{(18)} = 11.36$, $p < 0.05$). **c**) Orientation-selectivity was revealed by the significant difference in VEP magnitude driven by the familiar (blue, 289.83 ± 24.53μV) and novel stimulus (red, 166.86 ± 19.34 μV, 2-tailed paired t-test, $t_{(18)} = 10.081$, $p < 0.001$) on day-9. **d**) The vidget was significantly suppressed over the same time course as VEPs were potentiated, indicating habituation (n = 19; Friedman 1-way repeated measures ANOVA on ranks, $X^2_{(7)} = 25.13$, $p < 0.001$). This suppression was also significant by day-2 (3.24 ± 0.51 a.u.) relative to day-1 (4.14 ± 0.55 a.u.; Student-Newman-Keuls post-hoc test, $q_{(18)} = 6.49$, $p < 0.05$). Behavioural suppression saturated by day-8 (1.51 ± 0.15a.u.; Student-Newman-Keuls post-hoc test, $q_{(18)} = 6.28$, $p < 0.05$). **e**) Habituation was revealed to be orientation-selective on day-9 when the novel stimulus (red, 3.21 ± 0.43 a.u.) elicited vidgets of significantly greater magnitude than the familiar (blue, 1.61 ± 0.23 a.u.; n = 19; 2-tailed paired t-test, $t_{(18)} = -3.28$, $p = 0.004$). Throughout figure error bars are S.E.Ms and asterisks denote significance of $p < 0.05$.

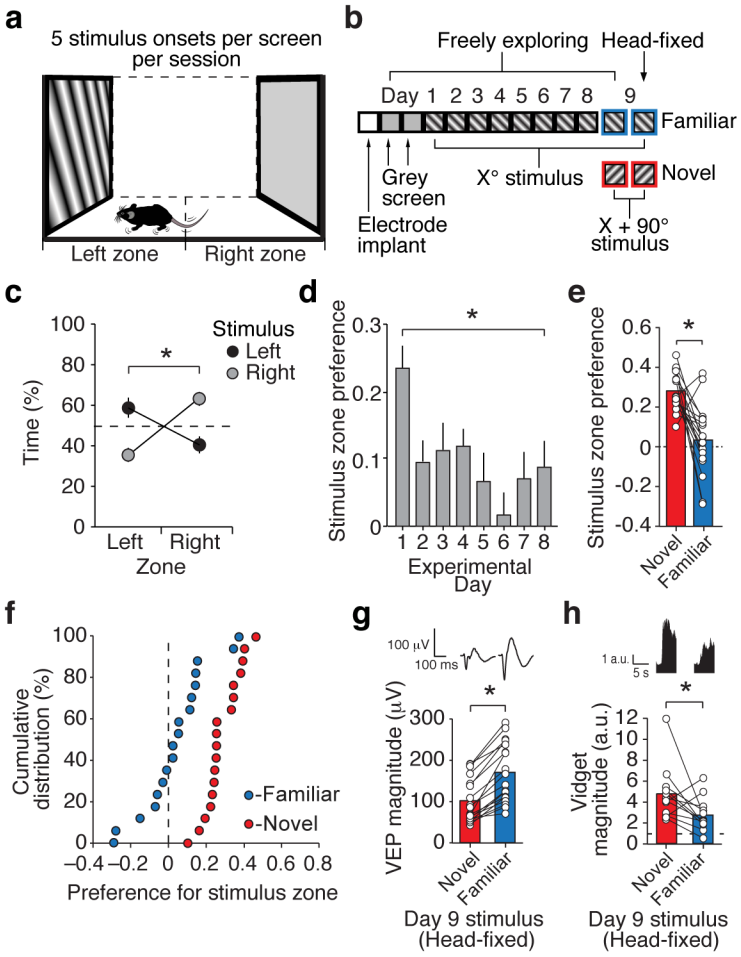

Figure 5. Freely moving mice explore sinusoidal grating stimuli, resulting in OSH

a) Mice (n = 18) explored a 40 cm x 40 cm arena with stimulus monitors at each end. **b**) Mice were habituated to the arena in 15-minute sessions during which static grey stimuli were presented on both monitors. Five blocks of a sinusoidal grating stimulus (X°) were then presented on each monitor (not simultaneously) on each of the next 8 days. On day-9, 5 blocks each of the familiar (X°) and a novel (X + 90°) oriented stimuli were presented on each monitor in order to test for OSH. Note that mice were habituated to the head-fixation apparatus without visual stimulation on days 7 and 8, 3–4 hours after free exploration. **c**) On day-1, the mice spent significantly more "active time" (velocity > 5cm/s) within the zone closest to stimulus presentation (i.e. left zone when stimulus was shown on the left monitor, etc.), indicating stimulus exploration (between subjects interaction: stimulus x zone: $F_{(1,68)} = 48.23$, $p < 0.001$). Mice spent more time exploring proximal to stimulus presentation, whether on the left (black, 59.5 ± 0.97 %) or right (grey, 64.1 ± 0.73 %). **d**) Stimulus zone preference, quantified by the difference in time spent exploring the zones proximate and distal to stimulus presentation divided by the total exploration time, decreased significantly over days (1-way repeated measures ANOVA: $F_{(7,119)} = 3.43$, $p = 0.002$, demonstrating habituation. **e–f)** On day-9, there was a significant effect of stimulus location and orientation on exploration (within-subjects 3-way interaction: Orientation x location x zone; $F_{(1,68)} =$

28.92, $p < 0.001$). Mice exhibited preference for the novel orientation (red, between subjects interaction: Location x zone; $F_{(1,68)} = 78.89$, $p < 0.001$) irrespective of stimulus location (i.e. on the left (65.8 ± 0.69 %) or the right (59.4 ± 0.65 %) of the arena). No significant preference was observed for the familiar stimulus (blue, between subjects interaction: Location x zone: $F_{(1,68)} = 1.95$, $p = 0.167$) on the left (50.9 ± 0.77 %) or the right (53.1 ± 0.60 %). Overall, there was greater preference (Paired t-test: $t_{(17)} = -4.51$, $p < 0.001$) for the novel (red, 0.28 ± 0.09) than the familiar stimulus (blue, 0.03 ± 0.17). **g–h**). In the head-fixed condition following free exploration, the familiar stimulus evoked significantly larger VEPs (blue, 169.2 ± 71.4 μV) than the novel stimulus (red, 100.8 ± 53 μV; n = 18; paired t-test: $t_{(17)} = 8.78$, $p < 0.001$), demonstrating the occurrence of SRP. In addition, the novel stimulus elicited significantly larger vidgets (red, 4.79 ± 0.76 a.u.) than the familiar stimulus (blue, 2.77 ± 0.46 a.u.; paired t-test: $t_{(11)} = 2.295$, $p = 0.042$), recorded in a subset of mice (n = 12), indicative of OSH. Throughout figure error bars are S.E.Ms and asterisks denote significance of $p < 0.05$.

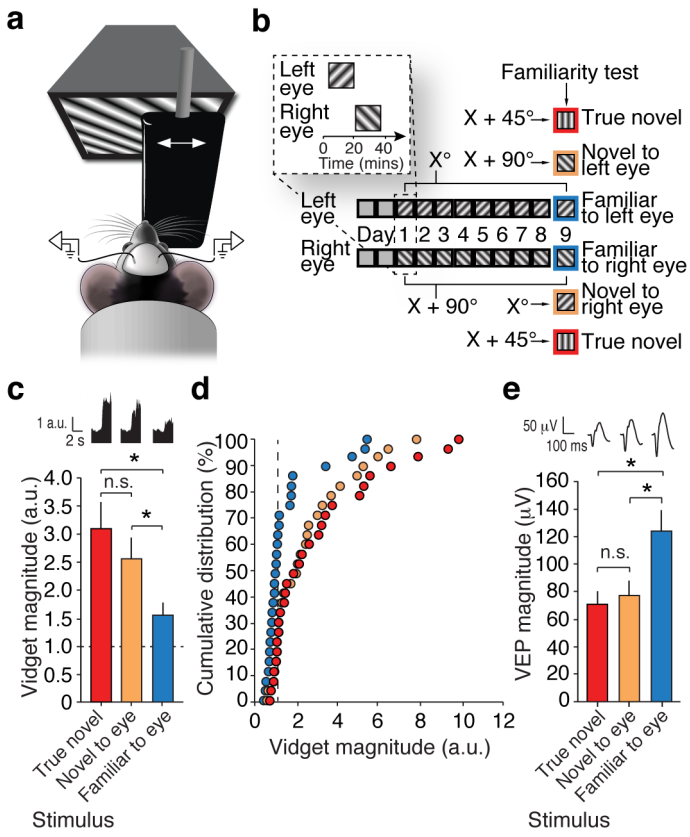

Figure 6. Orientation-selective habituation (OSH) is eye-specific

a) Presentation of full-field visual stimuli was limited to just one eye using an occluder. VEPs driven through the viewing eye were recorded in contralateral V1 while also recording vidgets. **b**) 14 mice were implanted bilaterally with VEP electrodes. On recovery they became accustomed to the recording apparatus for 2 days. A phase reversing sinusoidal grating stimulus was then selectively presented to the left eye only (X°). The orthogonal oriented stimulus was presented to the right eye only (X + 90°). Five stimulus blocks were delivered each day to each eye over 8 days. On day-9, each eye viewed the stimulus presented only to that eye for the previous 8 days as well as the stimulus viewed only by the opposing eye. A second novel stimulus, which had never been viewed by either eye, was also presented (X + 45°, here called 'true novel'). Five blocks of each stimulus were interleaved during this session. **c**) OSH is eye-specific as revealed on day-9 (n = 28 eyes from 14 mice). The stimulus familiar to an eye elicited vidgets of significantly lower magnitude (blue, 1.54 ± 0.26 a.u.; n = 28 eyes; Friedman 1-way repeated measures ANOVA on ranks, $X^2_{(2)} = 14.72$, $p < 0.001$) than the stimulus novel to the eye but familiar to the opposite eye (orange, 2.58 ± 0.36 a.u.; Student-Newman-Keuls post-hoc test, $q_{(27)} = 6.55$, $p < 0.05$) or the true novel stimulus (red, 3.10 ± 0.50 a.u.; Student-Newman-Keuls post-hoc test, $q_{(27)} = 4.73$, $p < 0.05$). There was no significant difference between the averaged magnitude of vidgets elicited by a stimulus novel only to the eye (orange) and the true novel stimulus (red, Student-Newman-Keuls post-hoc test, $q_{(27)} = 0.13$, n.s.). **d**) The cumulative distribution of average vidget magnitude elicited through each eye by the familiar (blue circles), novel only to eye (orange circles) and true novel stimulus (red circles) on day-9

shows that OSH is reliably eye specific. **e**) VEPs in response to the stimulus familiar to the eye elicited VEPs of significantly greater magnitude (blue, 124.21 ± 15.29 μV; n = 28 hemispheres; Friedman 1-way repeated measures ANOVA on ranks, $X^2_{(2)} = 26.74$, $p < 0.001$) than either true novel (red, 70.70 ± 9.71 μV; Student-Newman-Keuls post-hoc test, $q_{(27)} = 6.48$, $p < 0.05$) or novel-to-eye (orange, 77.02 ± 10.89 μV; Student-Newman-Keuls post-hoc test, $q_{(27)} = 8.65$, $p < 0.05$). There was also no significant difference between VEPs driven by the stimulus novel to the eye (orange) and true novel (red, Student-Newman-Keuls post-hoc test, $q_{(27)} = 0.52$, n.s.). Throughout figure error bars are S.E.Ms, asterisks denote significance of $p < 0.05$ and non-significant comparisons are denoted with n.s.

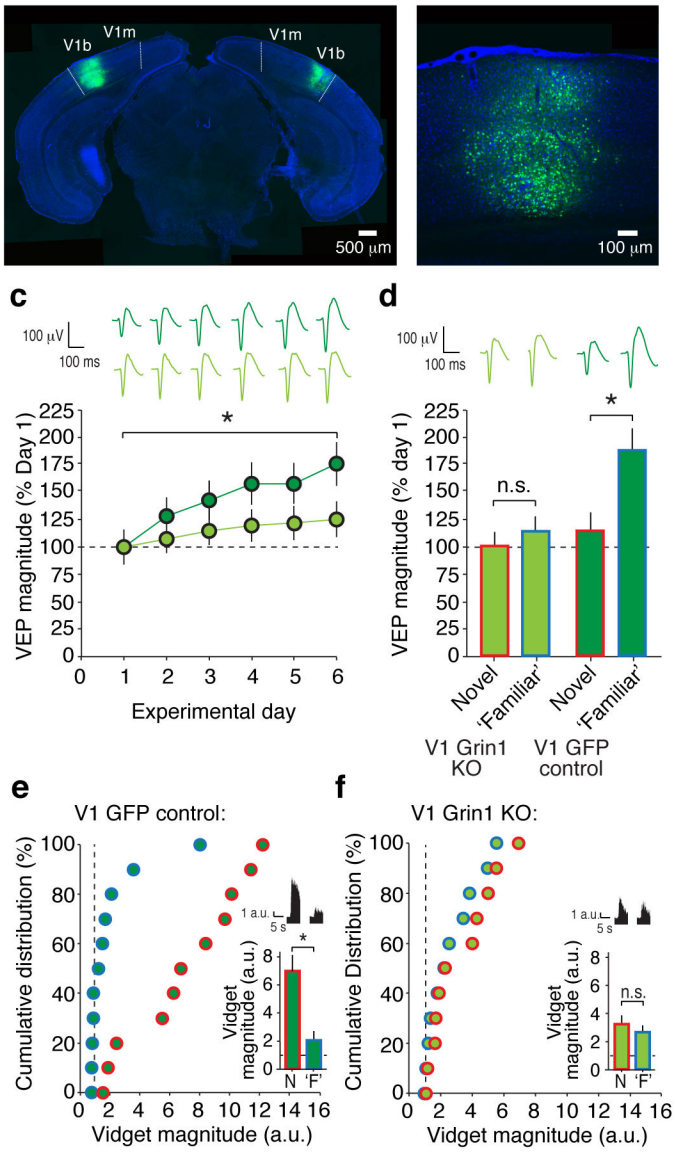

Figure 7. NMDA receptors in V1 are required for induction of OSH

a) NMDA receptors were locally ablated bilaterally in V1 of GRIN1$^{fl/fl}$ mice by locally expressing Cre recombinase through infection with an AAV8 virus. A GFP tag reveals the local spread of infection in V1, targeting the lateral binocular portion (V1b) and not the medial monocular region (V1m). **b**) Littermate GRIN1$^{fl/fl}$ mice locally expressing just GFP through infection with a matched AAV8 viral vector served as controls. **c**) SRP induction was significantly deficient in 11 Cre-expressing GRIN1$^{fl/fl}$ mice (light green circles) relative to interleaved littermate GFP only-expressing GRIN1$^{fl/fl}$ mice (dark green circles, 2-way repeated measures ANOVA: treatment x day interaction: $F_{(1,263)} = 5.523$; $p < 0.001$). **d**) Failure of SRP induction (ANOVA: treatment x stimulus interaction: $F_{(1,87)} = 25.634$; $p < 0.001$) is reflected by the equal magnitude of VEPs driven by novel (red outlines, 100.84 ± 12.95 % baseline) and familiar stimuli (blue outlines, 113.73 ± 14.57 baseline), in Cre-expressing GRIN1$^{fl/fl}$ mice (light green bars; n = 22 hemispheres; Student-Newman-Keuls

post-hoc test, $q_{(21)} = 2.142$, $p = 0.137$) during the final session familiarity test. Normal selectivity between novel (red outlines, 115.01 ± 14.58 % baseline) and familiar stimuli (blue outlines, 188.83 ± 19.40 % baseline) was observed in GFP only-expressing $GRIN1^{fl/fl}$ mice (dark green bars, n = 22 hemispheres; Student-Newman-Keuls post-hoc test, $q_{(21)} = 12.268$, $p < 0.001$) during interleaved test sessions. Averaged VEPs are shown at the top of panels **c–d. e**) OSH was similarly selectively blocked by knocking down NMDAR function in V1 (2-way repeated measures ANOVA: treatment x stimulus interaction: $F_{(1,43)} = 8.615$; $p = 0.008$). The cumulative distributions of average vidget magnitude per mouse driven by familiar (blue outlines, 2.03 ± 0.65 a.u.) and novel stimuli (red outlines, 6.92 ± 1.15 a.u.) in GFP only-expressing $GRIN1^{fl/fl}$ control mice (dark green), reveal consistent suppressive effect of familiarity (n = 11 mice; Student-Newman-Keuls post-hoc test, $q_{(10)} = 6.643$, $p < 0.001$), reflecting OSH. **f**) Vidgets of similar magnitude were evoked by familiar (blue outlines, 2.64 ± 0.48 a.u.) and novel stimuli (red outlines, 3.21 ± 0.61 a.u.; n = 11 mice; Student-Newman-Keuls post-hoc test, $q_{(10)} = 0.773$, $p = 0.591$) after deletion of GRIN1 in V1 (light green), demonstrating blockade of OSH. Average vidgets are presented at top of insets in panel **e–f**. Dashed lines represent pre-stimulus baseline for panels **e–f**. Throughout figure error bars are S.E.Ms, asterisks denote significance of $p < 0.05$ and non-significant comparisons are denoted with n.s.

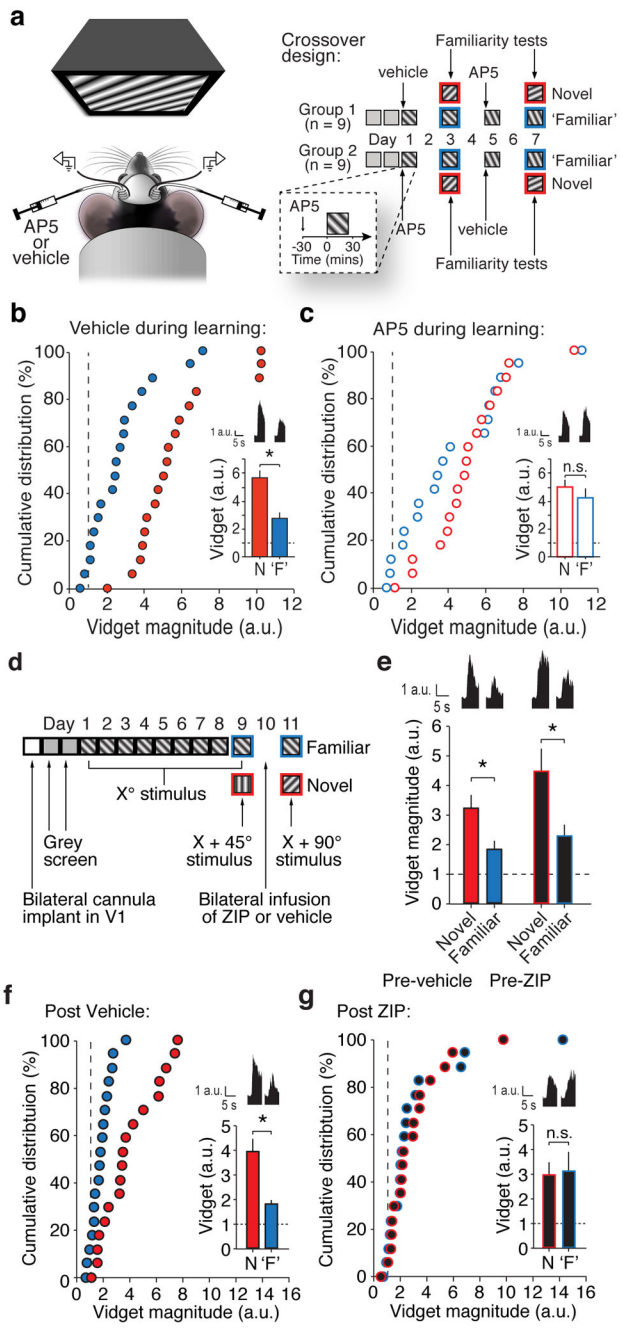

Figure 8. Local blockade of learning and erasure of memory in V1

a) Either the selective NMDAR antagonist AP5 (5 nMol in 1 μl over 10 minutes) or vehicle was infused bilaterally 30 minutes prior to stimulus onsets into binocular V1 of mice bilaterally implanted with injection cannulae and VEP recording electrodes. Mice were separated into 2 groups of 9 for a crossover experimental design. **b**) OSH occurred selectively after vehicle treatment but not AP5 treatment (2-way repeated measures ANOVA; n = 18; $F_{(1,17)} = 7.794$, p = 0.013). The cumulative distributions of average vidget per mouse driven by familiar (blue circles, 2.72 ± 0.43 a.u.) and novel stimuli (red circles, 5.59 ± 0.56 a.u.) after vehicle treatment, reveal consistent suppressive effect of familiarity

(Student-Newman-Keuls post-hoc test, $q_{(17)} = 4.82$, $p = 0.002$). **c**) After AP5 treatment, cumulative distributions of average vidget per mouse driven by previously viewed 'familiar' stimulus (blue circles, 4.16 ± 0.68 a.u.) and the novel stimulus (red circles, 4.97 ± 0.52 a.u.) are largely overlapping (n = 18) and, inset, no significant difference was observed (Student-Newman-Keuls post-hoc test, $q_{(17)} = 1.36$, $p = 0.34$). **d**) After saturation of OSH, 1 group of 18 mice were infused bilaterally with ZIP (10 nMol ZIP in 1 μl over 10 minutes) while another group of 18 mice were bilaterally infused with vehicle through infusion cannulae implanted bilaterally in binocular V1. This experiment revealed that OSH was susceptible to erasure by ZIP (3-way ANOVA, interaction of treatment x session x stimulus: $F_{(1,136)} = 4.27$, $p = 0.041$). **e**) Prior to infusions, OSH was expressed (n = 18; 2-way repeated measures ANOVA, effect of stimulus: $F_{(1,34)} = 11.80$, $p = 0.002$) and did not differ across treatment (treatment x stimulus: $F_{(1,34)} = 0.52$, $p = 0.48$). Prior to infusions of ZIP on day-9 (black bars), vidgets of significantly greater magnitude were observed in response to the novel stimuli (red outlines, 4.47 ± 0.81 a.u.) than the familiar (blue outlines, 2.32 ± 0.40 a.u.: Student-Newman-Keuls post-hoc test, $q_{(17)} = 4.16$, $p = 0.006$), reflective of OSH. **f**) On day-11, after infusions, a difference between the groups emerged (2-way repeated measures ANOVA, treatment x stimulus: $F_{(1,34)} = 4.63$, $p = 0.039$). On day-11, discrimination between novel and familiar stimuli was still present in the vehicle control group. Cumulative distributions of average vidget per mouse after vehicle infusions show separated distributions for familiar (blue, 1.81 ± 0.18 a.u.) and novel stimuli (red, 3.96 ± 0.50 a.u.) and, inset, this difference was statistically significant (Student-Newman-Keuls post-hoc test, $q_{(17)} = 4.00$, $p = 0.008$). **g**) In contrast, after ZIP infusions cumulative distributions of average vidget per mouse overlapped for familiar (blue, 3.17 ± 0.76 a.u.) and novel stimuli (red, 3.01 ± 0.53 a.u.) and, inset, any difference was not statistically significant (Student-Newman-Keuls post-hoc test, $q_{(17)} = 0.31$, $p = 0.830$). Dashed lines represent pre-stimulus baseline. Scale bar is 5 seconds horizontally and 1 a.u. vertically. Throughout figure error bars are S.E.Ms, asterisks denote significance of $p < 0.05$ and non-significant comparisons are denoted with n.s.